Characterisation of sawtooth instability at COMPASS

M. Imrisek[1,2], V. Weinzettl[1], F. Jaulmes[1], K. Bogár[1,2], J. Seidl[1], M. Tomes[1,2], P. Bílková[1], M. Hron[1]

email: imrisek@ipp.cas.cz

[1] Institute of Plasma Physics of the CAS, v.v.i., Za Slovankou 1782/3 182 00 Prague 8, Czech Republic
[2]Faculty of Mathematics and Physics, Charles University, Prague, V Holesovickach 2, CZ-180 00 Prague 8, Czech Republic

SAWTOOTH INSTABILITY

- Periodic appearance of internal kink mode vanishing during subsequent magnetic reconnection [1]
- Observed as sawtooth pattern on several diagnostics (electron temperature, soft X-rays)
- Routinely observed on COMPASS soft X-ray diagnostics [2] where SXR signal ~ $Z_{eff} n_e^2 \sqrt{T_e}$ + radiation of heavy impurities (complex dependence on T_e)
- Longer sawteeth period shown to trigger neoclassical tearing modes below the threshold for NTMs [3] →
- degradation of confinement
- Limits gradient of pressure and current profiles in plasma core
- Helps to remove impurities from plasma core
- Sawtooth instability changes temperature profile and magnetic topology in significant volume of plasma, and therefore affects various plasma processes

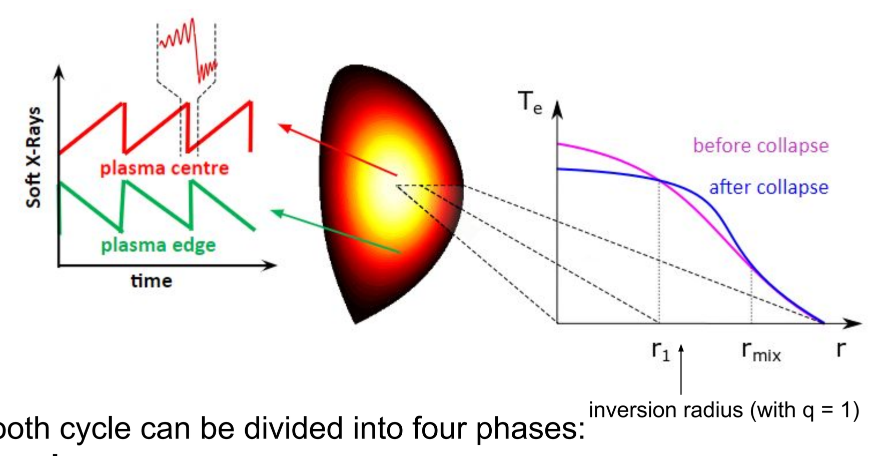

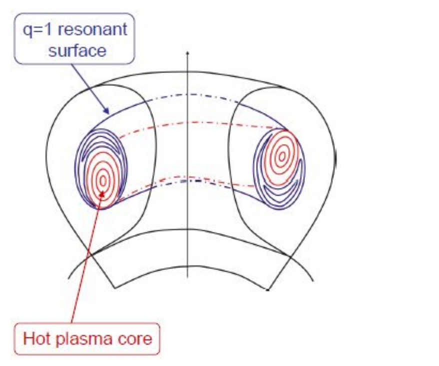

Displacement of hot plasma core during **internal kink mode** [4]

- A sawtooth cycle can be divided into four phases:

ramp-up phase
- gradual increase of temperature and its gradient in plasma core
- → high conductivity → higher j in plasma core → higher B_Θ → q < 1

pre-cursor phase
- necessary condition: q < 1
- development of internal kink instability (**m=1, n=1 mode**)
- displacement of plasma core - can be treated by energy principle:
- there is also critical pressure leading to the instability of kink mode $\delta\hat{W} = \delta\hat{W}_{\rm MHD} + \delta\hat{W}_{\rm trapped} + \delta W_{fast}$

fast collapse, resp. sawtooth crash
- magnetic reconnection (typically less than 100us in tokamaks)
- start of the reconnection often treated as Sweet-Parker, later more complex
- heat pulse from plasma core to the edge
- widely accepted model for sawtooth crash trigger: Porcelli model [5]

post-cursor phase
- oscillations indicating incomplete reconnection
- sometimes observed during NBI heating at COMPASS
- diamagnetic effects halting reconnection [6, 7]
- vanishes during relaxation processes

Safety factor (windines, resp. pitch of magnetic field): $q \simeq \frac{rB_z}{R_0 B_\theta}$

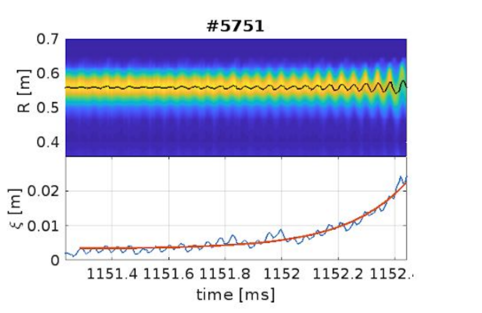

Exponential growth of plasma core displacement (seen by SXR tomography) during internal kink mode

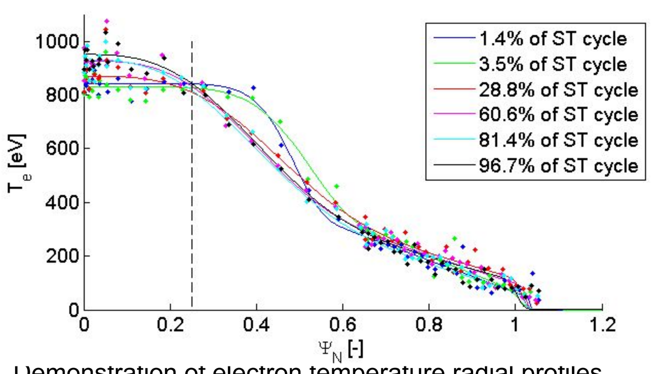

Demonstration of electron temperature radial profiles measured by Thomson scattering diagnostic during the different phases of sawtooth at COMPASS (#7690)

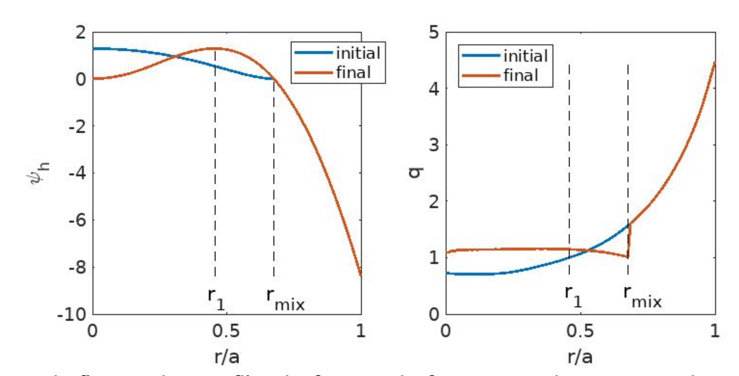

Helical magnetic flux and q-profiles before and after magnetic reconnection with respect to the radial profile normalised by minor radius according to the Kadomtsev model for shot #7690. The initial profiles were given by METIS simulation.

EFFECT OF SAWTOOTH ON EDGE PROCESSES

- **L-H transition** mostly appears within the first 20% of the sawtooth period (about 0.4ms after the L-H transition)

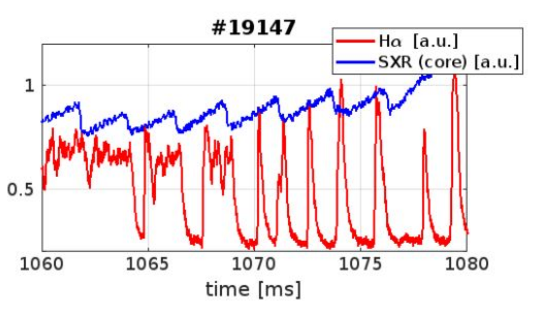

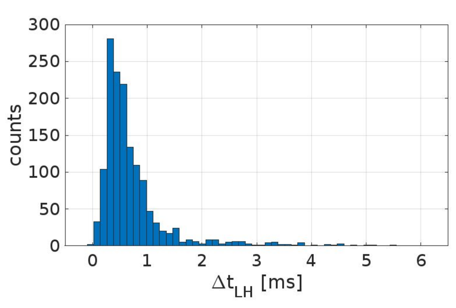

- **H-L transition** is mostly avoided within the first 30% of the sawtooth phase

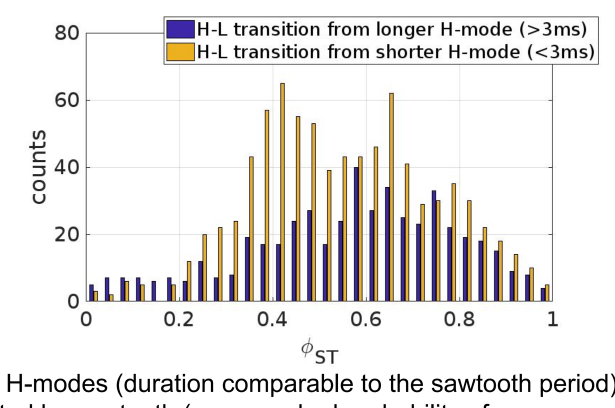

Shorter H-modes (duration comparable to the sawtooth period) strongly modulated by sawtooth (more peaked probability of occurrence, triggered shortly after the sawtooth crash and ending usually at ~ 40% of sawtooth phase (when the effect of the heat pulse and conditions at plasma edge are not sustainable for the H-mode).

- **Transition to ELM-free H-mode** coinciding with saw-tooth crashes (top) and applied NBI power with β_N (normalised ratio of kinetic and magnetic pressure) from EFIT (bottom)

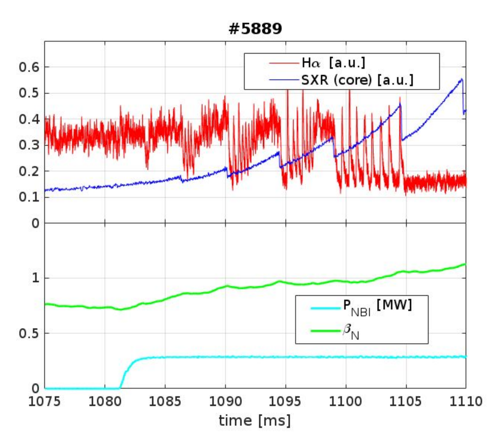

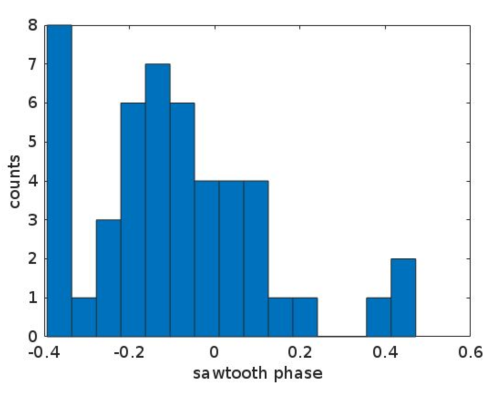

Occurrence of last ELMs before ELM-free H-mode phases with respect to the sawtooth phase

- **ELM distribution** drops at ~ 20% of sawtooth phase, resp. 0.4 ms after the sawtooth crash

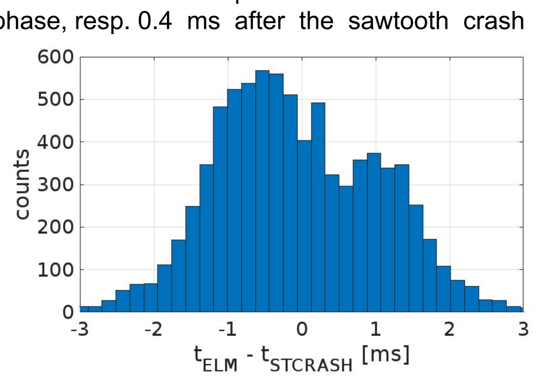

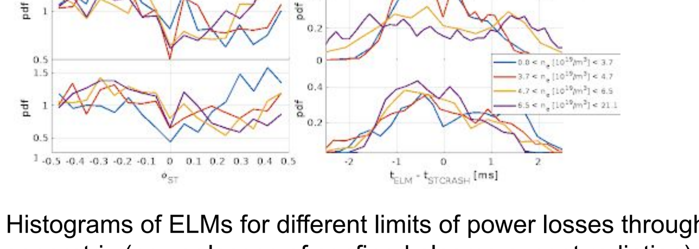

Histograms of ELMs for different limits of power losses through separatrix (power losses of confined plasma except radiation) P_{SEP}, electron density n_e

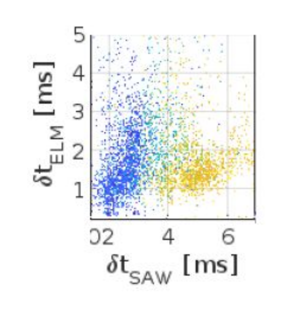

Sawtooth and elm period. Colors represent different P_{SEP}

SAWTOOTH PERIOD

- Sawtooth period - time required to reach the criteria for sawtooth crash, i.e. kink instability.
- When diffusion of current into plasma core is dominant mechanism (typically large sawtooth): $T_{SAW} \sim$ resistive time $= \mu a r_1 \sim T_e^{3/2}$
- When pressure gradient and other effects play a role [5]: $T_{SAW} \sim \tau_E$

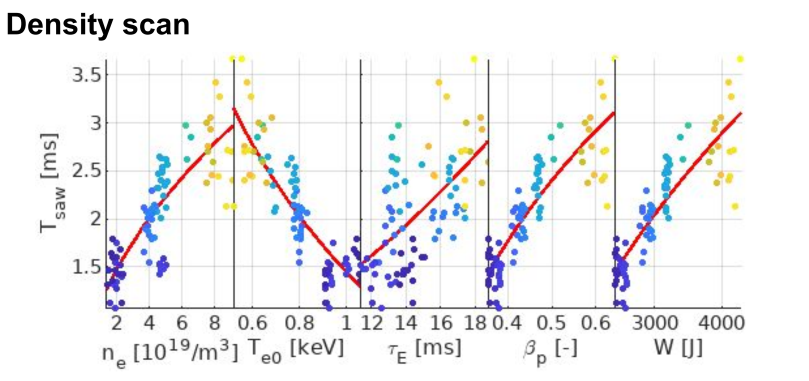

Sawtooth period (T_{SAW}) with respect to the electron density (n_e), central temperature (T_{e0}), energy confinement time (τ_E), ratio of kinetic pressure and pressure of poloidal magnetic field (β_p) and plasma energy (from EFIT). Colors represent electron density.

Effect of NBI

NBI influences plasma rotation (gyroscopic stabilization) and distribution of fast particles changing potential energy of kink mode and its stability

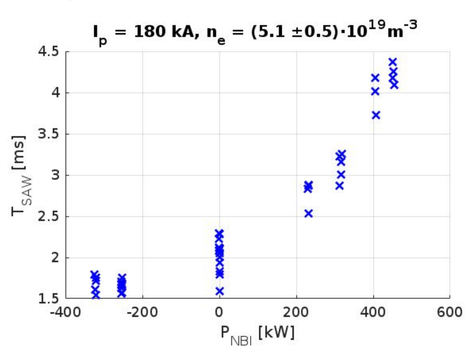

Sawtooth period with respect to applied NBI power reaches minimum at low level of counter-NBI. Higher counter-NBI induced other MHD instabilities avoiding sawteeth.

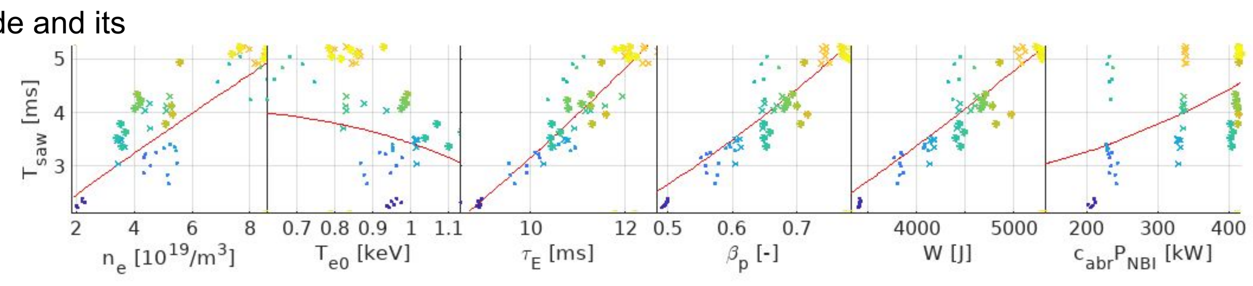

Sawtooth period during scan over plasma density and applied NBI heating is proportional to energy confinement time (τ_E)

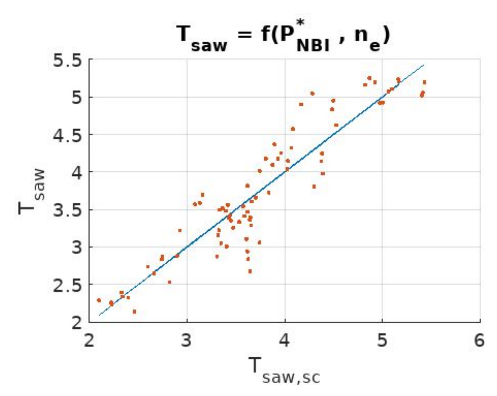

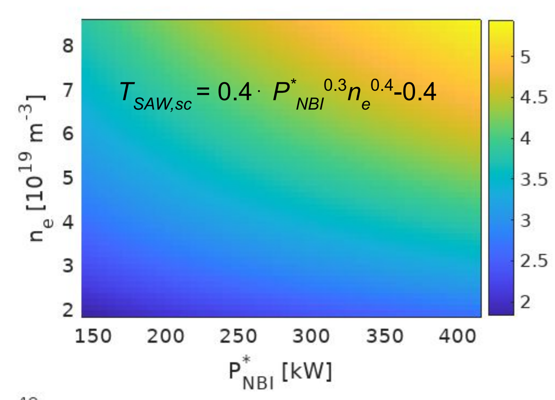

Scalings of sawtooth period during NBI scan as a function of plasma density and NBI power (right)

Note: At JET and MAST - minimum of sawtooth period at applied small counter-NBI due to competition of stabilising effects of trapped fast particles and flow shear [8]
At TEXTOR - minimum at low level of co-NBI due to gyroscopic stabilisation of the kink mode and the destabilisation arising in the presence of counter-passing fast ions [8]

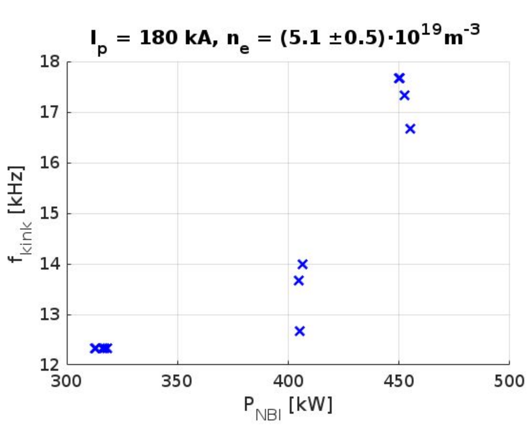

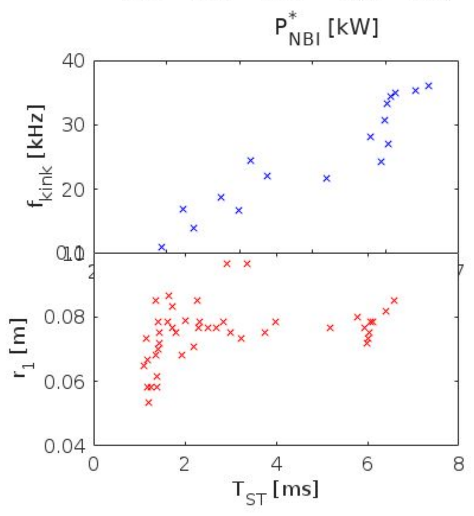

Internal kink mode frequency with respect to applied NBI and sawtooth period (right) indicating increase of toroidal plasma rotation.

H-mode vs L-mode

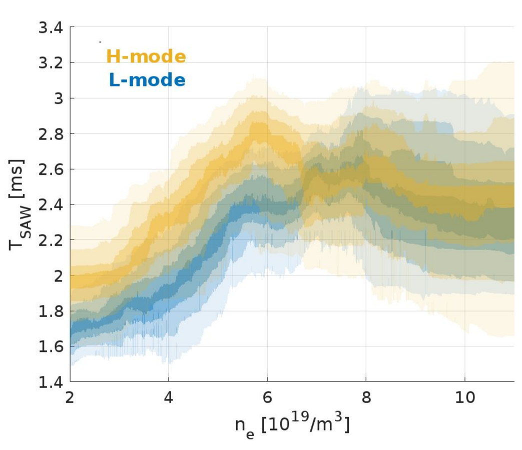

Dependence of sawtooth period on electron density during L-mode and H-mode. For higher densities, sawtooth period starts to decrease.

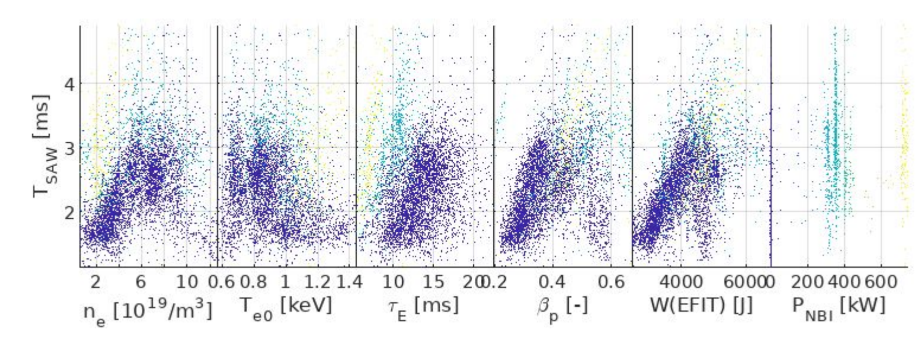

Sawtooth period (T_{SAW}) with respect to the electron density (n_e), central temperature (T_{e0}), energy confinement time (τ_E), ratio of kinetic pressure and pressure of poloidal magnetic field (β_p) and plasma energy (from EFIT). Colors represent electron density.

INVERSION RADIUS

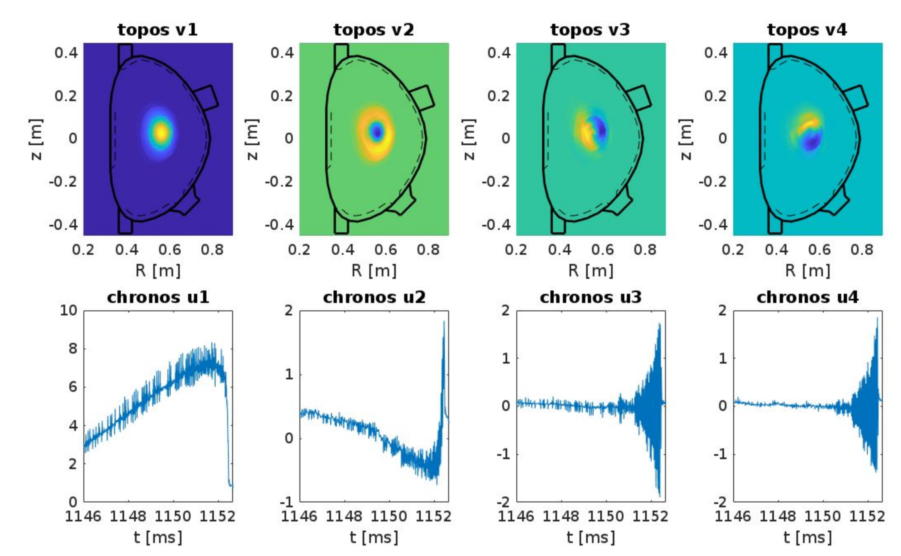

SVD applied on reconstructed SXR profiles during sawtooth crash neighbourhood in pulse #5751. Top row show modes whereas the bottom row shows their weight in time. First column correspond to the basic mode showing increase in core radiation followed by fast drop during sawtooth crash. Second column illustrates redistribution of radiation near inversion radius.Third and fourth columns correspond to oscillations caused by internal mode.

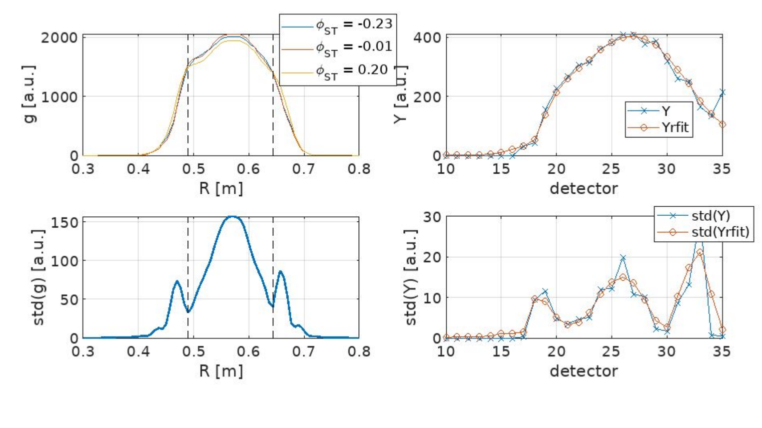

Reconstructed SXR profile (top-left), Variance of profiles (bottom-left), signals and retrofit (top-right) and its variation (bottom-right)

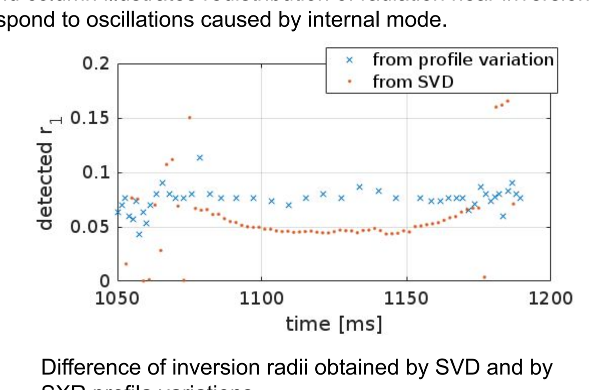

Difference of inversion radii obtained by SVD and by SXR profila variations

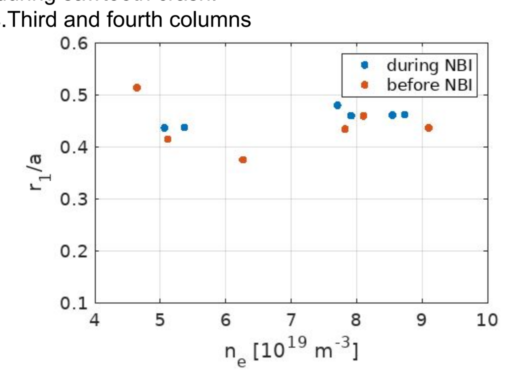

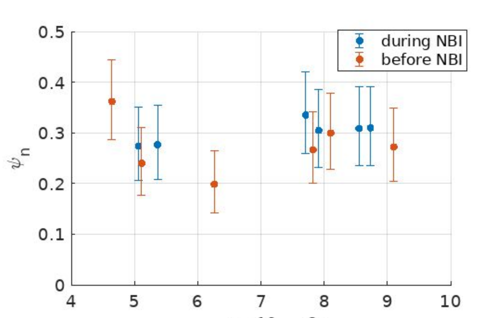

Inversion radius normalised to minor radius (left) and as normalised poloidal flux (right) before (red) and after (blue) NBI heating (with 10-12 A and 40 kV). Change of inversion radius below resolution of SXR tomography

SUMMARY

- Sawtooth period increases with NBI and decreases with temperature, i.e. resistive time (effects like pressure gradient or magnetic shear may play a role)
- Change of inversion radius during NBI below spatial resolution of SXR detectors
- Sawtooth crash triggers L-H transition, avoids H-L transition (especially for shorter H-modes) and suppress occurence of ELMs

EUROPEAN UNION
European Structural and Investment Funds
Operational Programme Research, Development and Education

MINISTRY OF EDUCATION, YOUTH AND SPORTS

Acknowledgement

This work has been carried out within the framework of the project COMPASS RI - Research (No. CZ.02.1.01/0.0/0.0/16_013/0001551) and co-funded from European structural and investment funds.

References

[1] S. Goeler, W. Stodiek, and N. Sauthoff., *Phys. Rev. Letters*, 33(20):1201–1203, Nov 1974.
[2] M. Imrisek et al. *Rev. of Sc. Inst.*, 2014, 85(11)
[3] D. J. Campbell et al, *Phys. Rev. Lett.*, 1988
[4] W. M. Stacey. *Fusion plasma physics*. Wiley-VCH, 2012
[5] F. Porcelli et al. *Plasma Phys. and Contr. F.* 38(12), Jan 1996
[6] M. Swisdak et al. *Jour.l of Geophys. Res.*: Space Physics, 108(A5), 2003.
[7] M. T. Beidler and P. A. Cassak. *Phys. Rev. Lett.*, 107(25), 2011.
[8] I.T. Chapman et al, 2011, *Plasma Phys. Contr. F.* 53 013001